Received: 13 April 2022 | Revised: 25 May 2022 | Accepted: 10 June 2022

DOI: 10.1096/fj.202200573R

THE FASEB JOURNAL

RESEARCH ARTICLE

Lysyl oxidase promotes renal fibrosis via accelerating collagen cross-link driving by β-arrestin/ERK/STAT3 pathway

Xiaoqin Zhang[1] | **Wenqian Zhou**[1] | **Yangyang Niu**[1] | **Saiya Zhu**[1] | **Yingying Zhang**[1] | **Xiaogang Li**[2,3] | **Chen Yu**[1]

[1]Department of Nephrology, Shanghai Tongji Hospital, Tongji University School of Medicine, Shanghai, China

[2]Department of Internal Medicine, Mayo Clinic, Rochester, Minnesota, USA

[3]Dpartment of Biochemistry and Molecular Biology, Mayo Clinic, Rochester, Minnesota, USA

Correspondence
Chen Yu, Department of Nephrology, Shanghai Tongji Hospital, Tongji University School of Medicine, 389 Xincun Road, Shanghai 200065, China.
Email: yuchen@tongji.edu.cn

Funding information
Foundation for the National Institutes of Health (FNIH), Grant/Award Number: R01 DK 129241 and R01 DK126662; National Natural Science Foundation of China (NSFC), Grant/Award Number: 82170696 and 81873609

Abstract

Lysyl oxidase (LOX) is a copper-dependent monoamine oxidase whose primary function is the covalent cross-linking of collagen in the extracellular matrix (ECM). Evidence has shown that LOX is associated with cancer and some fibrotic conditions. We recently found that serum LOX is a potential diagnostic biomarker for renal fibrosis, but the mechanism by which LOX is regulated and contributes to renal fibrosis remains unknown. The current study demonstrates the following: (1) LOX expression was increased in fibrotic kidneys including ischemia-reperfusion injury-(IRI-), unilateral ureteral obstruction-(UUO-), and folic acid- (FA-) induced fibrotic kidneys as well as in the paraffin-embedded sections of human kidneys from the patients with renal fibrosis. (2) The increasing deposition and cross-linking of collagen induced by LOX was observed in IRI-, UUO- and FA-kidneys. (3) LOX was regulated by the β-arrestin-ERK-STAT3 pathway in renal fibrosis. STAT3 was the downstream of AT1R-β-arrestin-ERK, ERK entered the nucleus and activated STAT3-pY705 but not STAT3-pS727. (4) STAT3 nuclear subtranslocation and binding to the LOX promoter may be responsible for the upregulation of LOX expression. (5) Pharmacologic inhibition of LOX with BAPN in vivo inhibited the upregulation of LOX, decreased collagen over cross-linking and ameliorated renal fibrosis after ischemic injury. Collectively, these observations suggest that LOX plays an essential role in the development of renal fibrosis by catalyzing collagen over cross-linking. Thus, strategies targeting LOX could be a new avenue in developing therapeutics against renal fibrosis.

Abbreviations: AngII, angiotensin II; ANS, hypertensive nephrosclerosis; AT1R, angiotensin II type I receptor; BAPN, β-aminopropionitrile; ChIP, chromatin immunoprecipitation; CKD, chronic kidney disease; DEGs, differentially expressed genes; DN, diabetic nephropathy; ECM, extracellular matrix; ERK, extracellular regulated protein kinases; FA, folic acid; GPCRs, G protein-coupled receptors; IRI, ischemia-reperfusion injury; Lcn2, neutrophil gelatinase-associated lipocalin; LOX, lysyl oxidase; MAPK, mitogen-activated protein kinase; MN, membranous nephropathy; MCD, minimal change disease; NRK-52E, rat renal tubular epithelial cells; qRT-PCR, quantitative reverse-transcription polymerase chain reaction; RTK, receptor tyrosine kinase; SII, angiotensin II peptide analog [Sar, Ile (4), Ile (8)]; Timp1, tissue inhibitor of metalloproteinases-1; UUO, unilateral ureteral obstruction.

KEYWORDS
ERK/STAT3, LOX, renal fibrosis, STAT3-pY705, β-arrestin pathway

1 | INTRODUCTION

Renal fibrosis is an indispensable pathophysiological feature of renal aging and chronic kidney disease (CKD) irrespective of etiology and is characterized by the excess accumulation of extracellular matrix (ECM) substances.[1,2] The pathogenesis of renal fibrosis engages multiple molecular pathways and almost all kidney resident cells and infiltrating cells. Despite substantial progress over the years in understanding the mechanisms of renal fibrosis, there is still a lack of sufficient therapies to treat or prevent renal fibrosis in clinical settings thus far.

Fibrosis is the result of a series of molecular and cellular events, including fibroblast activation and/or proliferation and the transcriptional induction of collagens. The extracellular matrix (ECM) remodeling is particularly prevalent during fibrosis, leading to functional changes in biochemical and biomechanical properties of ECM.[3] Lysyl Oxidase (LOX) is an amine oxidase with both intracellular and extracellular functions, which plays an important role in diverse biological processes and diseases.[4] The alteration of LOX activity or expression makes changes in the cellular microenvironment, leading to many diseases, including cancer, atherosclerosis, and inflammatory diseases.[4,5] In cancers, overexpression of LOX is involved in several processes of the tumorigenic pathways, resulting in the enhancement of cancer cell proliferation, invasion, metastasis, and angiogenesis in different cancer types and stages. Thus, LOX becomes an emerging therapeutic target for cancer treatment.[6,7] The activation of LOX has also been associated with chronic fibrotic disorders, including fibrotic pulmonary[8] and liver fibrosis,[9] and genetic or pharmacologic disruption of LOX can attenuate fibrogenesis in those organs by inhibition of fibrotic activation of myofibroblasts. We recently show that serum LOX is a potential diagnostic biomarker for renal fibrosis.[10] However, little is known about the molecular mechanism of LOX regulation in renal fibrosis.

G protein-coupled receptors (GPCRs) are the largest family of cell-surface receptors[11] and mainly rely on heterotrimeric guanine nucleotide-binding proteins (G proteins)–mediated receptor phosphorylation, which is involved in nearly every aspect of mammalian life and play a fundamental role in angiogenesis, hormone release, neurotransmission, and immune surveillance.[12] Angiotensin II type I receptor (AT1R) is a GPCR that plays a central role in kidney diseases.[13] β-arrestin is a family of cytoplasmic scaffolding proteins that regulate GPCR signal transduction and consists of 2 members, ARRB1 and ARRB2.[14] Recently, accumulating evidence together with our previous study indicates that β-arrestin not only acts as a negative adaptor of GPCRs[15,16] but also regulates a diverse array of cellular functions independent of GPCR activation,[13,17,18] which has been known as β-arrestin biased pathway.[19] We found that β-arrestin signaling plays a much more important role than G protein signaling in angiotensin II (Ang II)-induced renal fibrosis.[20] β-arrestin activation is responsible for signal transduction through extracellular signal-regulated protein kinase (ERK1/2) and eventually leads to the development of renal fibrosis.[20–22] However, the downstream targets of β-arrestin-ERK and their roles in the process of renal fibrosis remain poorly understood.

In this study, we investigated the mechanism of LOX regulation in the β-arrestin signaling pathway in renal fibrosis both in vivo and in vitro and identified the role of ERK-STAT3 activation in the β-arrestin pathway. We also evaluated the effect of pharmacological inhibition of LOX on renal fibrosis in the IRI induced renal fibrosis model. We found that inhibition of LOX attenuates renal fibrosis by decreasing collagen cross-linking and limiting collagen deposition, suggesting that LOX is a potential therapeutic target for the treatment of renal fibrosis.

2 | METHODS

2.1 | Cell culture and reagents

Normal rat kidney tubule epithelial cells (NRK-52E cells), and HEK-293 cells were cultured as described. Before the experiment, cells were starved overnight in a medium containing 0.5% FBS and then treated with drugs. AT1R-β-ARR biased agonist SII ([1-sar, 4, 8-ile]-angiotensin II) was purchased from Jill biochemical and dissolved in ddH_20 at a stock solution of 10 mM. Angiotensin II human was purchased from Sigma-Aldrich (cat# 4474-91-3). PD98059 was purchased from Selleck (cat# 167869–21-8).

The antibodies used for Western blot analysis included (a) anti- LOX (no. 31238), anti-β-arrestin1 (no. 32099), anti-elastin (no. 21610), anti-Col1 (no. 34710), and anti-GAPDH (no. 82451), purchased from Abcam; (b) anti- ERK1/2 (no. 4695), and anti-p-ERK1/2 (no. 4370), purchased from Cell Signaling Technology; and (c) anti -STAT3 (sc-482), anti-STAT3-pS727 (no. sc-800R) and anti-STAT3-pY705 (sc-7993) were purchased from Santa Cruz Biotechnology Inc. The secondary antibodies, including donkey anti-rabbit IgG–horseradish

peroxidase (sc-2313), and goat anti-mouse IgG–horseradish peroxidase (sc-2005) were purchased from Santa Cruz Biotechnology Inc.

2.2 | Animal model and treatments

Ischemia-reperfusion injury (IRI) mode1: Male C57BL/6J mice (6–8 weeks old, weighing 20–25 g, SLRC laboratory Animal, Shanghai, China) were subjected to IRI model and were anesthetized with 3% sodium pentobarbital solution (0.009 ml/g, Sigma, USA) by intraperitoneal injection. The left renal pedicle was clamped with an atraumatic vascular clip for 45 min through a flank incision and the left kidney turned purple subsequent to clamping. Clamps were removed after 45 min to start reperfusion and the left kidney reverted to red within approximately 10 s. The muscle layer and skin were closed with 4–0 silk sutures. Sham animal models were subjected to a similar surgical procedure without clamping the left kidney pedicle. The animal received the irreversible inhibitor of LOX activity BAPN (100 mg/kg/day: Sigma Aldrich, USA), or vehicle continuously for 28 days by gavage.

Unilateral urethral obstruction (UUO) model: Male Sprague Dawley (SD) rats (200–250 g, SLRC laboratory Animal, Shanghai, China) were subjected to sham or UUO. Each group consisted of at least 6 rats and UUO was performed as previously described.

Folic acid (FA)-treated models: Male C57BL/6J mice (6–8 weeks old, weighing 20–25 g, SLRC Laboratory Animal, Shanghai, China) were injected with a single dose of folic acid (FA) (250 mg/kg dissolved in 0.3 M $NaHCO_3$) or vehicle intraperitoneally.

All experiments in animals were reviewed and approved by the ethics committee of Tongji University School of Medicine and were performed in accordance with the institutional guidelines.

2.3 | Patients and tissue specimens

Tissue samples, including both para-carcinoma tissues and renal biopsies. Para-carcinoma tissues were collected during surgical operations and at least 2 cm distant from the edge of the cancerous mass. Renal biopsies were performed as a part of a routine clinical diagnostic investigation and collected according to the pathological diagnosis of fibrosis score. These investigations were conducted in accordance with the principles of the Declaration of Helsinki and were approved by the Research Ethics Committee of Tongji Hospital after informed consent was obtained from the patients.

2.4 | Western blot analysis

Cell pellets of kidney tissue were collected and resuspended in lysis buffer (20 mM Tris–HCl, pH 7.4150 mM NaCl, 10% glycerol, 1% Triton X-100, 1 mM Na3VO4, 25 mM β-glycerolphosphate, 0.1 mM PMSF, Roche complete protease inhibitor set, and Sigma-Aldrich phosphatase inhibitor set). The resuspended cell pellet was vortexed for 20 s and then incubated on ice for 30 min and centrifuged at 20 000 *g* for 30 min. The supernatants were collected for western blot analysis.

Nuclear plasma separation: Cultured cell lysates were prepared using commercial kits (Beyotime, #P0027) according to the manufacturer's protocol.

2.5 | Quantitative reverse-transcription polymerase chain reaction (qRT-PCR)

Total RNA was extracted using the RNeasy Plus Mini Kit (QIAGEN). Total RNA (1 μg) was used for RT reactions in a 20-μl reaction to synthesize cDNA using an iScript cDNA Synthesis Kit (Bio-Rad). RNA expression profiles were analyzed by real-time PCR using iTaq SYBR Green Supermix with ROX (Bio-Rad) in an iCycler iQ Real-Time PCR Detection System. The complete reactions were subjected to the following program of thermal cycling: 40 cycles of 10 s at 95°C and 20 s at 60°C. A melting curve was run after the PCR cycles, followed by a cooling step. Each sample was run in triplicate in each experiment, and each experiment was repeated 3 times. Expression levels of target genes were normalized to the expression level of actin. All primers used are listed in Table 1.

2.6 | Histology and immunofluorescence staining

Paraffin-embedded sections (4 μm) were subjected to H&E staining, and Masson's trichrome to detect interstitial fibrosis, using commercial kits (Solarbio) according to the manufacturer's protocol. Kidney sections were counterstained by hematoxylin. Images were analyzed using a Nikon Eclipse 80i microscope.

2.7 | Immunofluorescence staining

For STAT3 staining, a rabbit anti-STAT3 antibody (sc-482; Santa Cruz Biotechnology Inc.) and Alexa Fluor 488 anti-rabbit IgG secondary antibody were used. Images were analyzed using a Nikon Eclipse 80i microscope.

TABLE 1 The primers used for quantitative real-time PCR and ChIP-PCR

Genes	Forward primers (5′-3′)	Forward primers (5′-3′)
GAPDH (rat)	GGCAAGTTCAACGGCACA	CCATTTGATGTTAGCGGGAT
β-arrestin1 (rat)	CTGGATGTCTTGGGTCTGA	CATTGACGCTGATGGGTT
LOX (rat)	CATTACCACAGCATGGATGAAT	CAGTCTATGTCTGCTGCATAAG
STAT3 (rat)	GAGGAGGCATTCGGAAAG	TCGTTGGTGTCACACAGAT
GAPDH (mouse)	AAGGTCGGTGTGAACGGATT	CGCTCCTGGAAGATGGTGAT
LOX (mouse)	ATATAGGGGCGGATGTCAGAG	CGAATGTCACAGCGTACAAC
β-arrestin1 (mouse)	ACCTTTGAGATCCCGCCAAA	CAGGGGCATACTGAACCTTC
LOX promoter-NC	CTGGAAATCAGTCTGGAGGTTC	AACATAGGAGCACGTGTC
LOX promoter	GAGGGCTCAGTGGTTAAGAC	CAGCCATTATGTGGGTACAAAG

2.8 | RNA interference

The RNA oligonucleotides that specifically targeted rat STAT3, β-arrestin1 were purchased from GenePharma (Shanghai, China). The RNA oligonucleotides were transfected with the Dharma-FECT siRNA transfection reagent (Dharmacon). After siRNA transfection for 24 or 48 h, cells were harvested and analyzed by western blotting and qRT-PCR.

2.9 | Chromatin immunoprecipitation (ChIP) assay

ChIP assay was performed according to the protocol described.[23] Chromatin DNA was subjected to immunoprecipitation with anti-STAT3, or normal rabbit IgG, and then washed, after which the DNA-protein cross-links were reversed. The recovered DNA was analyzed by PCR for the binding of STAT3 at the rat LOX promoter.

2.10 | Collagen cross-linking

Kidney collagen was fractionated into pepsin-soluble and -insoluble parts, with the insoluble collagen being largely cross-linked. The renal tissue was dissociated by incubation in 0.5 mol/L acetic acids for 12 h and then treated with 5 mg/mL pepsin for 12 h. Pepsin-soluble and -insoluble collagens were separated by centrifugation at 3000 *g* for 10 min at 4°C. The two collagen fractions were hydrolyzed in a high-pressure tank and then quantified by measuring hydroxyproline using the modified Stegemann method.

2.11 | RNA-sequence

Total RNA of kidneys from mouse kidney or rat kidney tissues was extracted with TRIzol (Invitrogen, #15596026). The mRNA was purified from total RNA by an mRNA Purification Kit (Invitrogen, #61006) and was converted to double-stranded cDNA. The cDNA library was generated using the Collibri Stranded RNA Library Prep Kit (Invitrogen, #a38994024). All samples were sent to the GENEWIZ Technology Corporation (SuZhou), and an Illumina platform was used for mRNA sequencing.

RNA-Seq and Bioinformatics Analysis: Paired-end transcriptome reads were mapped to the mouse reference genome (GRCm38) using STAR spliced read aligner[24] and the count matrices were generated from reads aligned to the genome by the Rsubread package in R which contains the feature Counts function.[25] The count data of gene expression was normalized using the trimmed mean of *M*-values (TMM) using the edgeR package in R.[26] Differentially expressed genes between the sham and IR28d groups were determined using the R package edgeR, which implements an empirical Bayes method to estimate gene expression changes.

The R package gplots contain a heatmap.2 function was used to plot the heatmaps and implement hierarchical clustering. The network analysis of gene-pathway associations for DEGs was implemented using the cluster Profiler package in R.[27] Enrichment *p*-values were corrected using Benjamini and Hochberg procedure and the top 30 GO pathways ranked by adjusted *p*-values and their related DEGs were used to generate the gene-pathway network. The enrichment clustering test and transcription factor-target gene set enrichment were done with Metascape.[28] The GO or TRRUST terms with an enrichment *p*-value cutoff of .01 were clustered by Kappa similarities[29] among all pairs of terms.

2.12 | Statistical analysis

All data are presented as mean ± SEM. All statistical analyses were performed using SPSS Statistics 22

software. *p*-values were calculated by a two-tailed unpaired Student's *t*-test, and a *p*-value less than .05 was considered significant.

3 | RESULTS

3.1 | LOX expression is markedly elevated in fibrotic kidneys and is responsible for collagen over cross-linking

To identify the factor responsible for the pathogenesis of renal fibrosis, we performed RNA-seq analysis in FA-treated and UUO mouse kidney tissues. We identified 482 upregulated and 70 downregulated genes in the UUO mouse kidneys, and 801 upregulated and 302 downregulated genes in the FA-treated mouse kidneys across all comparisons (UUO vs. sham, FA vs. sham). There were 130 overlapping genes among the upregulated genes and 11 overlapping genes among the downregulated genes in these two kinds of fibrotic kidneys (Figure 1A). Among these overlapping genes, we identified 25 upregulated genes and 1 downregulated gene that were associated with fibrosis according to the fibro Atlas database (http://biokb.ncpsb.org/fibroatlas/) (Figure 1B). We showed the top 10 differentially expressed genes related to fibrosis in these two models, which included Lcn2 (neutrophil gelatinase-associated lipocalin), Timp1 (tissue inhibitor of metalloproteinases-1), and LOX genes (Figure 1C). For that the Lcn2 and Timp1 have been reported to be correlated with renal fibrosis,[30,31] we focused on the roles and mechanisms of LOX in renal fibrosis.

LOX is an extracellular copper-dependent monoamine oxidase that catalyzes the cross-linking of soluble collagen and elastin into insoluble, mature fibers.[32] As the first step toward understanding the role of LOX in renal fibrosis, we examined the expression of LOX in kidneys of patients with different diseases compared to normal kidneys (control) dissected from renal cancer patients by immunohistochemistry staining. As shown in Figure 1D, we observed an intense LOX labeling in both the cytosol and the nucleus of tubular cells and interstitial myofibroblasts in the fibrotic kidney. In contrast, the expression of LOX could only be detected in a few tubular epithelial cells but not in interstitial myofibroblasts in no fibrotic kidneys from para-carcinoma tissue or diagnosed with minimal change disease (MCD). We also examined the expression of LOX in a murine model of renal fibrosis induced by IRI, UUO, and FA, and found that LOX mRNA levels were significantly increased in fibrotic kidneys compared to sham groups (Figure S1A–C). Notably, after UUO injury, LOX mRNA was gradually increased over time, reaching the maximum level on day 14 (Figure S1B). Consistently, the protein level of LOX was also markedly increased in kidneys with IRI, UUO, and FA injury compared to sham group kidneys as examined by western blot (Figure 1E). For that LOX is well known for its role in ECM remolding, we measured the cross-linking of collagen in kidneys with IRI, UUO, and FA injury. We found that the overall ratio of insoluble collagen to soluble collagen in the IRI-, UUO-, and FA-treated (Figure 1F) kidneys was significantly higher than that in the sham-treated kidneys. Taken together, these results suggest that upregulation of LOX-mediated collagen cross-linking is associated with renal fibrosis.

3.2 | The β-arrestin-ERK pathway was activated in kidneys after IRI injury and cultured renal tubular epithelial cells

In neonatal cardiac fibroblasts, AngII could induce LOX expression and collagen cross-linking.[33] We and others reported that AngII-AT1R-β-arrestin-dependent signaling plays an important role in renal fibrosis induced by UUO.[13] To investigate whether the upregulation of LOX in renal fibrosis is regulated by AngII-AT1R-β-arrestin-dependent signaling, we examine the activation of β-arrestin-dependent signaling in the IRI injured kidney and cultured rat renal tubular epithelial cells (NRK-52E) in response to SII (angiotensin II peptide analog [Sar, Ile (4), Ile (8)]. SII is a selective agonist of β-arrestin, which mediates the stimulation of AT1R, leading to the activation of β-arrestin-mediated signaling pathways and renal fibrosis.[13] As indicated in Figure 2A,B, the mRNA and protein levels of β-arrestin-1 were increased significantly in kidneys in IRI models with the development of renal tubulointerstitial fibrosis. ERK (extracellular regulated protein kinases) is one of β-arrestin-mediated signaling components and the β-arrestin/ERK signal complex acts as a transducer to converge a variety of extracellular stimuli to intracellular signaling pathways.[30,34] As shown in Figure 2B, IRI injury led to an increase in the phosphorylation of ERK1/2 compared to sham-operated kidneys. To further demonstrate the activation of β-arrestin dependent signaling pathway in the regulation of LOX in renal fibrosis, NRK-52E cells were treated with SII. We found that the expression of β-arrestin1 and LOX mRNAs and proteins were upregulated in cultured NRK-52E cells treated with SII in a time-dependent manner (Figures 2C,D and S2A,B). Expectedly, treatment with SII also led to ERK1/2 entered the nucleus and further to be phosphorylated in NRK-52E cells (Figures 2E and S2A,B). These results suggest an association of the β-arrestin-ERK signaling pathway with the expression of LOX in the development of renal fibrosis.

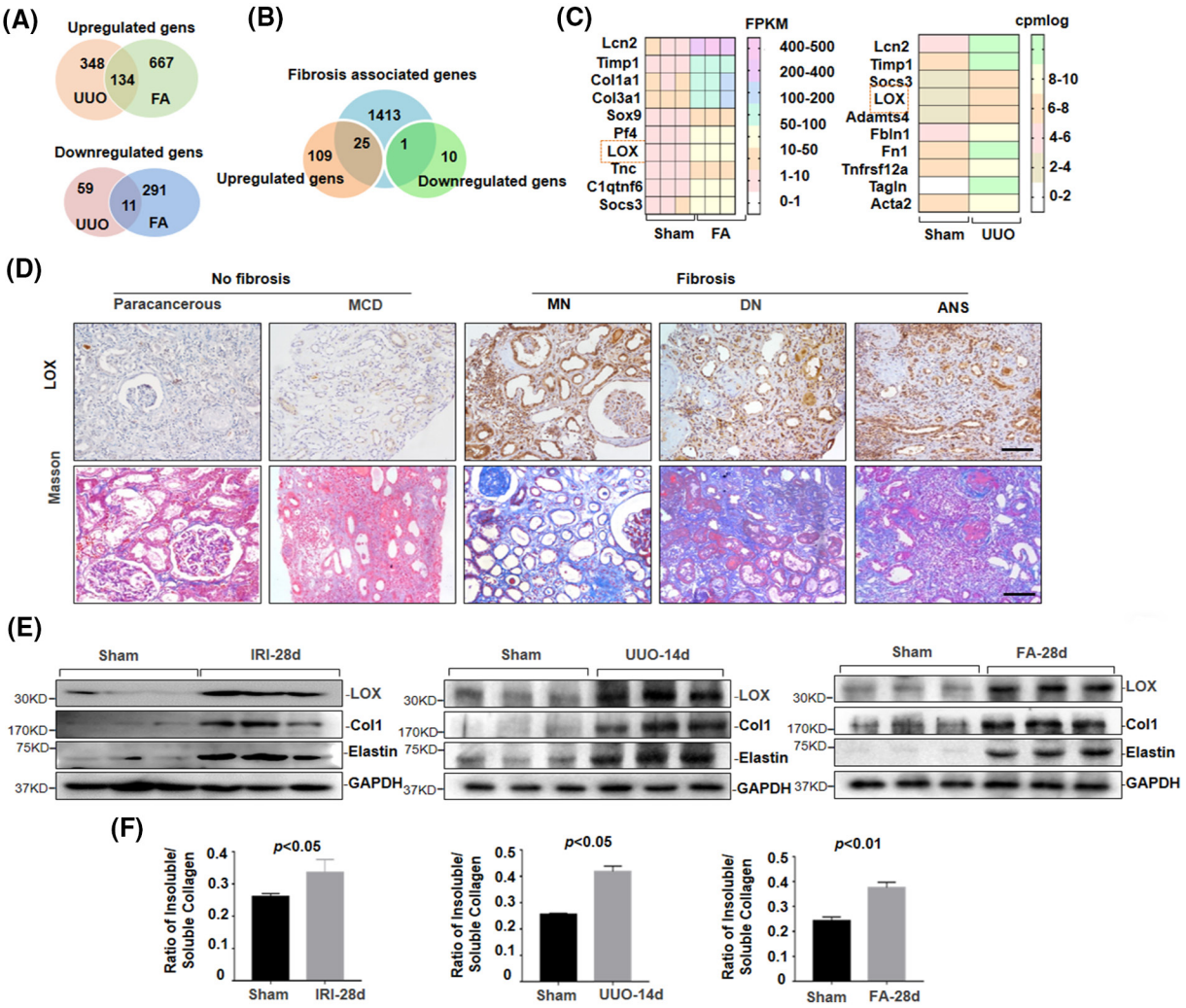

FIGURE 1 LOX expression is markedly elevated in fibrotic kidneys and responsible for collagen over cross-linking. (A) Venn diagram showing the number of up-regulated (Upper panel) or down-regulated genes (bottom panel) in UUO mice and FA-tread mice detected from bioinformatic analysis of RNA-seq data. (B)The number of fibrosis-associated gens detected from UUO mice and FA-tread mice overlap of up-regulated and down-regulated genes identified by RNA-seq. (C) Hierarchical clustering of the top 10 differential expression genes (DEGs) related fibrosis in these two models. The gene expression was quantified via RSEM v1.2.12 with the default options. The "value" stands for FPKM (FA-treated mice) and cpmlog (UUO mice) expression of DEG. (D) Representative images of immunostaining with LOX antibody in kidney sections from patients with and without renal fibrosis. (E) Western blot analysis of LOX, elastin, and Col1 levels in kidneys collected from IRI-, UUO- and FA- mice. (F) The ratio of insoluble/soluble collagen was analyzed in kidneys collected from IRI-, UUO- and FA-mice. ANS, hypertensive nephrosclerosis; DN, diabetic nephropathy; MCD, minimal change disease; MN, membranous nephropathy. Each bar represents the mean ± SEM for groups of at least 6 mice in vivo. The scale bar is 50 μm.

3.3 | STAT3 was activated by β-arrestin-ERK in the kidneys after IRI injury and cultured renal tubular epithelial cells

To further demonstrate the mechanism of β-arrestin-ERK-mediated pro-fibrotic cellular responses, we performed an RNA-seq analysis of renal tissues from the IRI model (Figure 3A). To better understand the inherent interaction among the differentially expressed genes (DEGs), we analyzed the gene-pathway association network based on the top-enriched pathways from the GO database. We identified a few key pathways involved in kidney fibrosis development, such as those of extracellular structure organization and myeloid leukocyte migration. Interestingly, we also found a pathway that responded to copper iron (Figure 3B). Aberrant activation of the transcriptional program of fibrogenic genes plays a prominent role in the pathogenesis of kidney fibrosis. To identify key transcriptional programs involved in disease etiology, we performed target gene enrichment analysis using the transcription factor-target gene interaction database TRRUST (transcriptional regulatory relationships unraveled by sentence-based text mining). We identified 8 transcriptional factor-mediated gene expression programs that

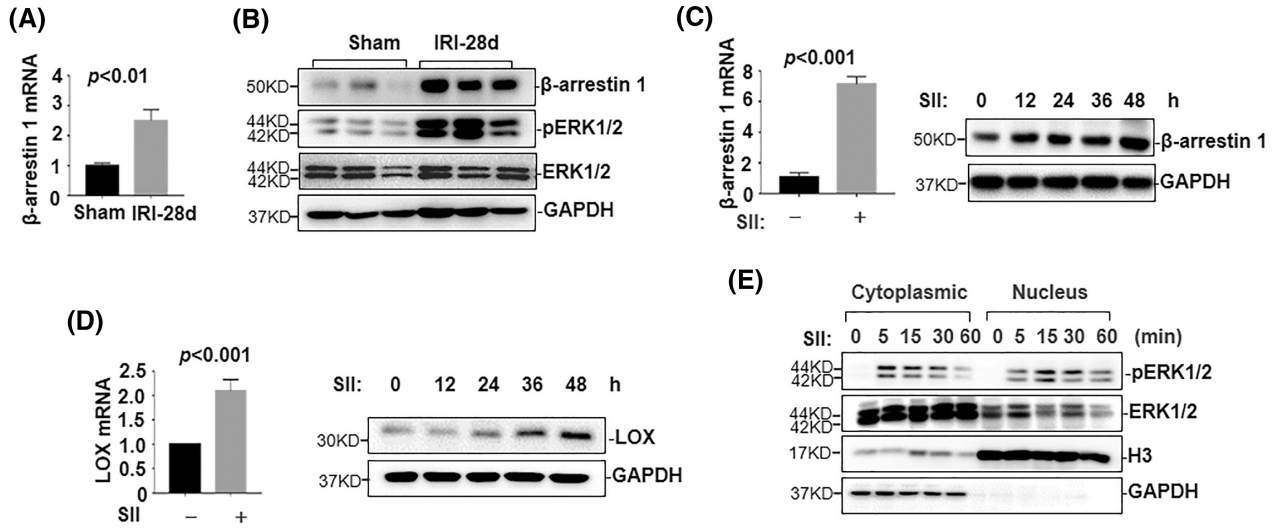

FIGURE 2 β-arrestin-ERK pathway was activated in the kidneys after IRI injury and cultured renal tubular epithelial cells. (A) qRT-PCR analysis of mRNA levels of β-arrestin1 in kidneys collected from mice with or without IRI injury. Each bar represents the mean ± SEM for groups of at least 6 mice in vivo. (B) Western blot analysis of the expression β-arrestin1 and the phosphorylation of ERK in kidneys collected from mice with or without IRI injury. (C) qRT-PCR analysis of the expression of β-arrestin1 in NRK-52E cells treated with SII for 24 h and Western blot analysis of the expression of β-arrestin1 in NRK-52E cells treated with SII for 0, 12, 24, 36 and 48 h. (D) qRT-PCR analysis of the expression of LOX in NRK-52E cells treated with SII for 24 h and Western blot analysis of the expression of β-arrestin1 in NRK-52E cells treated with SII for 0, 12, 24, 36 and 48 h. (E) Western blot analysis of the ERK and phosphorylation of ERK in cytoplasm and nucleus of NRK-52E cells treated with SII at indicated time point. Data are the means ± SEM; $n = 3$ biologically independent samples; unpaired two-tailed Student's *t*-test.

were significantly enriched in IRI- kidneys (Figure 3C), including Nfkb1, Jun, STAT3, Runx2, Ep300, Spi1, Cebpb, and Rfx5.

STAT3 is a transcription factor that regulates the transcription of target genes involved in many crucial physiological functions, including cell growth, proliferation, inflammation, and apoptosis.[31] To further investigate the role of STAT3 in renal fibrosis, we examined the phosphorylation levels of STAT3 in kidneys after IRI injury. We found that the phosphorylation of its tyrosine 705 (STAT3-pY705) and serine 727 (STAT3-pS727) residues were increased in IRI kidneys compared to sham kidneys (Figure 3D). To determine whether there is a link between STAT3 activation and β-arrestin-ERK signaling in renal fibrosis, we examined the activation of STAT3 in NRK-52E cells treated with SII or AngII. We found that the phosphorylation of STAT3 at Tyr705 and Ser727 increased NRK-52E cells in the presence of AngII (Figure S4A) but only increased the phosphorylation of STAT3 at Tyr705 in the presence of SII (Figures 3E and S3A). To validate that the activation of STAT3 is regulated by β-arrestin1, we further found that knockdown of β-arrestin1 with siRNA dramatically abrogated the activation of STAT3-pY705 (Figures 3F and S3B), supporting that β-arrestin1 is involved in the activation of STAT3. Notably, knockdown of β-arrestin1 also restored the phosphorylation of ERK induced by SII, which is in line with ERK activation in response to β-arrestin1 upregulation (Figures 3F and S3B). To further evaluate the role of β-arrestin-ERK signaling in STAT3-pY705 activation, NRK-52E cells were treated with the MEK inhibitor PD98059 for 30 min prior to SII treatment. We found that treatment with PD98059 not only blocked ERK activation but also inhibited the STAT3 activation at Tyr705 in response to SII (Figures 3G and S3C). Taken together, these results support that β-arrestin-ERK activation is essential for the activation of STAT3 in the kidney after injury and in culture renal tubular cells treated with SII.

3.4 | STAT3 nuclear sublocation is responsible for LOX transcriptional activation

To understand whether the expression LOX is regulated by STAT3 activation, first, we found that STAT3 was predominant nuclear localization in response to SII in cultured 293 T cells as examined with immunofluorescence staining (Figure 4A). We further found an increase in STAT3-pY705 in the nuclear fraction of NRK-52E cells treated with 10 μM SII, which reached a peak at 30 min of SII treatment, but no change was observed in the cytoplasmic fraction (Figure 4B). To assess fraction purity, we used histone H3 and GAPDH

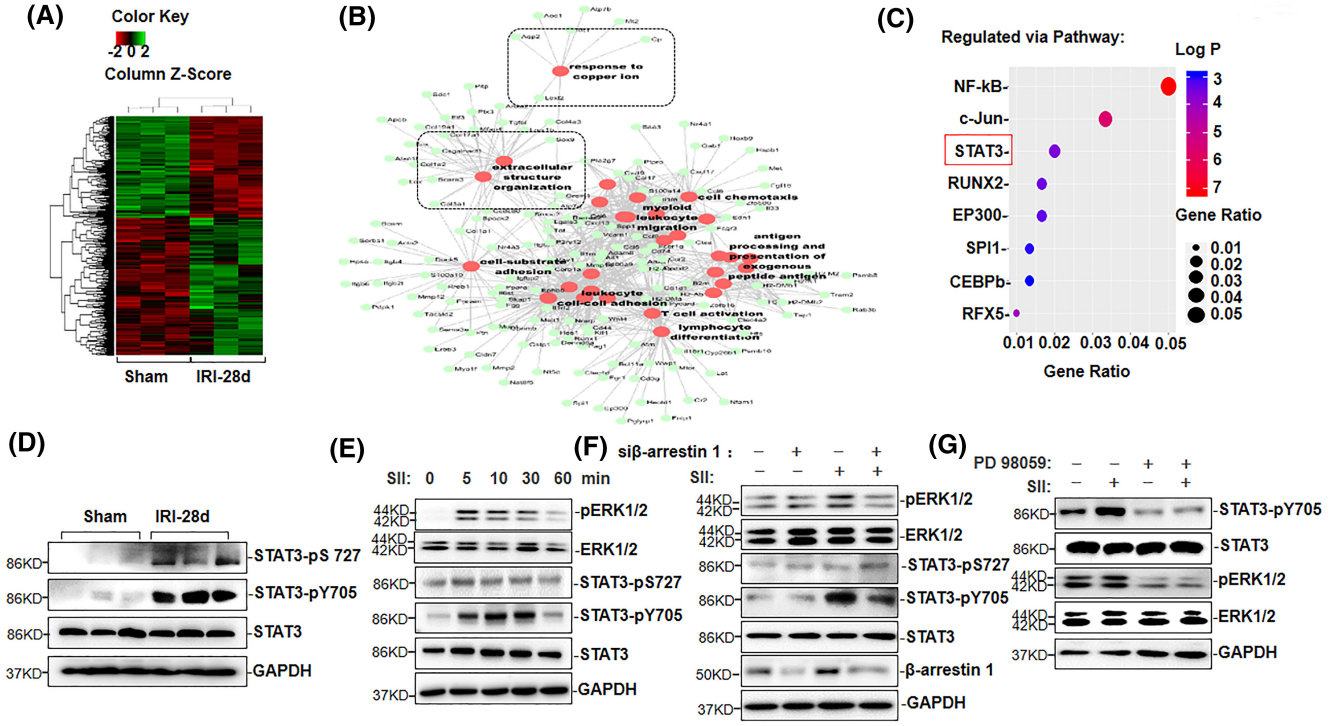

FIGURE 3 STAT3 was activated by β-arrestin-ERK in the kidneys after IRI injury and cultured renal tubular epithelial cells. (A) Heat map of the top significant DEGs (FDR ″0.1) with hierarchical clustering from IRI mouse kidneys RNA-seq data. (B) The gene-pathway association network is based on the top enriched pathways from the GO database using DEGs. (C) Target gene enrichment analysis of IRI mouse kidneys RNA-seq using TRRUST. (D) Western blot analysis of phosphorylation level of STAT3 in kidneys from mice with or without IRI injury. (E) Western blot analysis of the phosphorylation of ERK and STAT3 in NRK-52E cells treated with SII for 0, 5, 15, 30, and 60 min. (F) Western blot analysis of the expression and phosphorylation of ERK and STAT3 in NRK-52E cells transfected with β-arrestin1 siRNA for 48 h and then incubated with SII for an additional 30 min. (G) Western blot analysis of the expression and phosphorylation of ERK and STAT3 in NRK-52E cells in the presence of SII with or without PD98059 treatment.

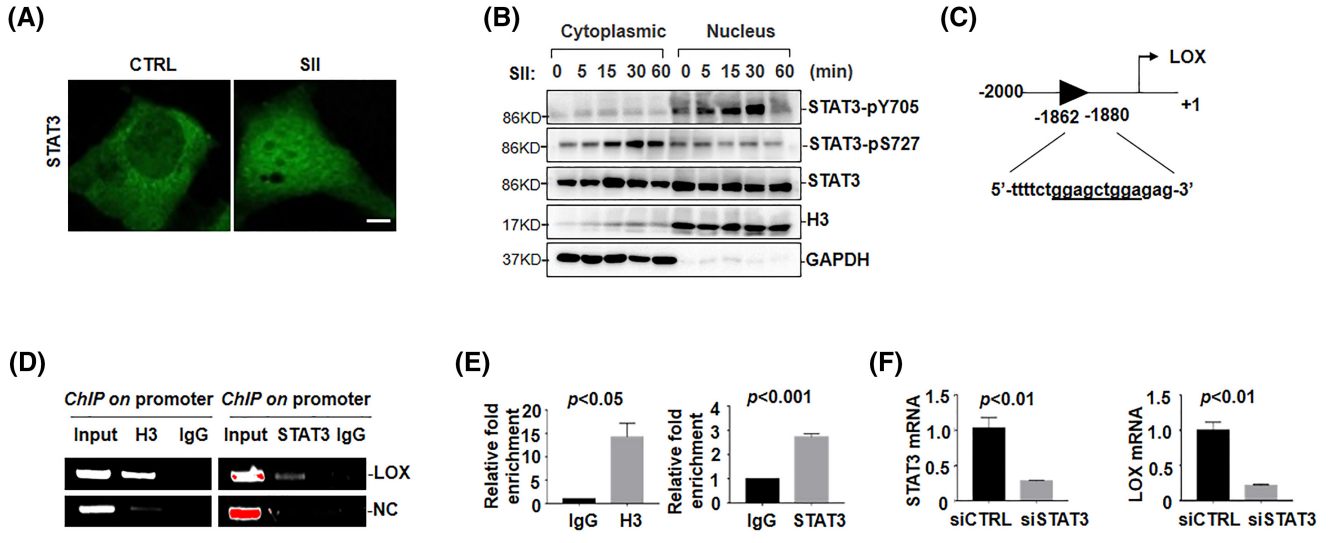

FIGURE 4 STAT3 nuclear sublocation is responsible for LOX transcriptional activation. (A) Representative images of immunostaining with STAT3 antibody in HEK 293 T cells treated with SII or vehicle. (B) Western blot analysis of the expression and phosphorylation of STAT3 in cytoplasm and nucleus of NRK-52E cells treated with SII (10 μM) at indicated time point. (C) The localization and the sequence of the STAT3-binding motif in the promoter of LOX. (D and E) ChIP (D) and ChIP-qPCR (E) analysis indicated that STAT3 is bound to the promoter of LOX in NRK-52E cells. Histone H3 was used as a positive control. Normal rabbit IgG was used as a negative control. (F) qRT-PCR analysis of the expression of LOX and STAT3 in NRK-52E cells transfected with STAT3 siRNA and mock siRNA for 48 h. Data are the means ± SEM; $n = 3$ biologically independent samples; unpaired two-tailed Student's *t*-test. The scale bar is 50 μm.

as markers of nucleus and cytoplasm, respectively. We also found that STAT3-pS727 was slightly increased in the cytoplasm but slightly decreased in the nucleus (Figure 4B). Moreover, we treated NRK-52E cells with AngII and found that the phosphorylation of STAT3 at Tyr705 and Ser727 was increased both in nuclear and cytoplasmic fraction (Figure S4B). These results demonstrate that the phosphorylation of STAT3 at Tyr705 rather than Ser727 is responsible for its nuclear localization in response to SII stimulation.

We next investigated whether STAT3 can bind to the promoter of LOX to regulate its transcription. A conserved STAT3 binding motif, 5′-GGAGCTGGA-3′, was identified in the LOX promoter in the LOX promoter (Figure 4C). The binding of STAT3 to the LOX promoter was confirmed in NRK-52E cells with a ChIP assay (Figure 4D,E). We further found that knockdown of STAT3 with siRNA decreased the expression of LOX in NRK-52E cells (Figure 4F). These results suggest that STAT3 functions as a transcriptional factor to regulate LOX expression in renal epithelial cells.

3.5 | LOX was regulated by the β-arrestin-ERK-STAT3 pathway and responsible for collagen over cross-linking

Given that LOX expression was regulated by STAT3 activation, we next investigated whether the expression of LOX depended on the β-arrestin-ERK-STAT3 pathway in cultured NRK-52E cells treated with SII. As indicated in Figure 5A, SII exposure resulted in an increase in the expression of LOX at both the mRNA and protein levels, whereas knockdown of β-arrestin-1 with siRNA suppressed SII-induced the expression of LOX (Figures 5B and S5A). In addition, MEK inhibitor PD98058 treatment also suppressed SII-induced the expression of LOX (Figures 5C and S5B). To further validate the β-arrestin-ERK-STAT3 pathway in mediating the LOX expression, we found that knockdown of STAT3 with siRNA largely suppressed the expression of LOX in NRK-52E cells treatment with SII (Figures 5D and S5C), which further support that STAT3 is responsible for LOX expression and dependence of β-arrestin-ERK pathway on this process. Altogether, these results suggest that LOX expression is regulated by the β-arrestin-ERK-STAT3 pathway.

3.6 | Targeting LOX using BAPN protects against renal fibrosis development

To assess the role of LOX in the development of renal fibrosis, we examined the effect of β-aminopropionitrile (BAPN) on IRI-induced renal fibrosis in mice. On day 28, after IRI with or without administration of BAPN, kidneys were collected and then subjected to Masson trichrome staining and immunoblot analysis of the expression of ECM proteins. We found that ECM proteins were extensively deposited within the interstitial of IRI injured kidneys (Figure 6A). A semiquantitative analysis indicated that Masson trichrome-positive areas of ECM

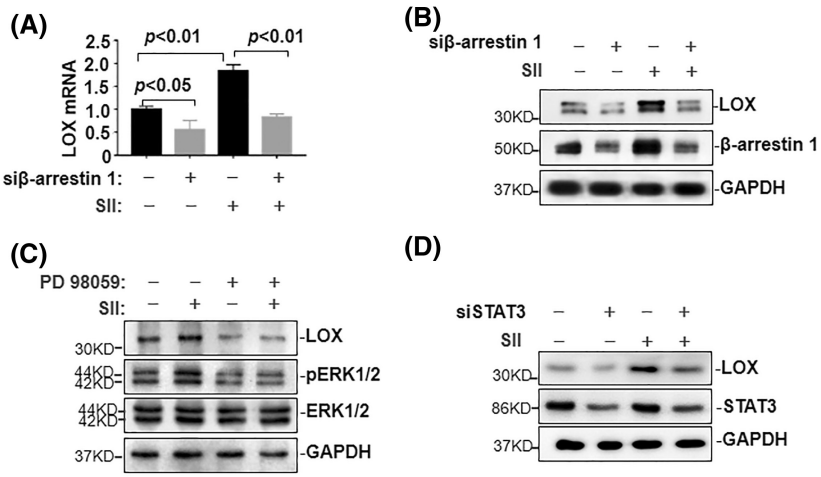

FIGURE 5 LOX was regulated by the β-arrestin-ERK-STAT3 pathway. (A) qRT-PCR analysis of the expression of LOX and β-arrestin1 in NRK-52E cells transfected with β-arrestin siRNA or mock siRNA for 48 h with or without SII treatment. (B) Western blot analysis of the expression of LOX and β-arrestin1 in NRK-52E cells transfected with β-arrestin siRNA or mock siRNA with or without SII treatment. (C) Western blot analysis of the expression LOX, p-ERK, and ERK in NRK-52E cells treatment with PD98059 with or without SII treatment. (D) Western blot analysis of the expression LOX and STAT3 in NRK-52E cells transfected with STAT3 siRNA or mock siRNA with or without SII treatment. Data are the means ± SEM; $n = 3$ biologically independent samples; unpaired two-tailed Student's *t*-test.

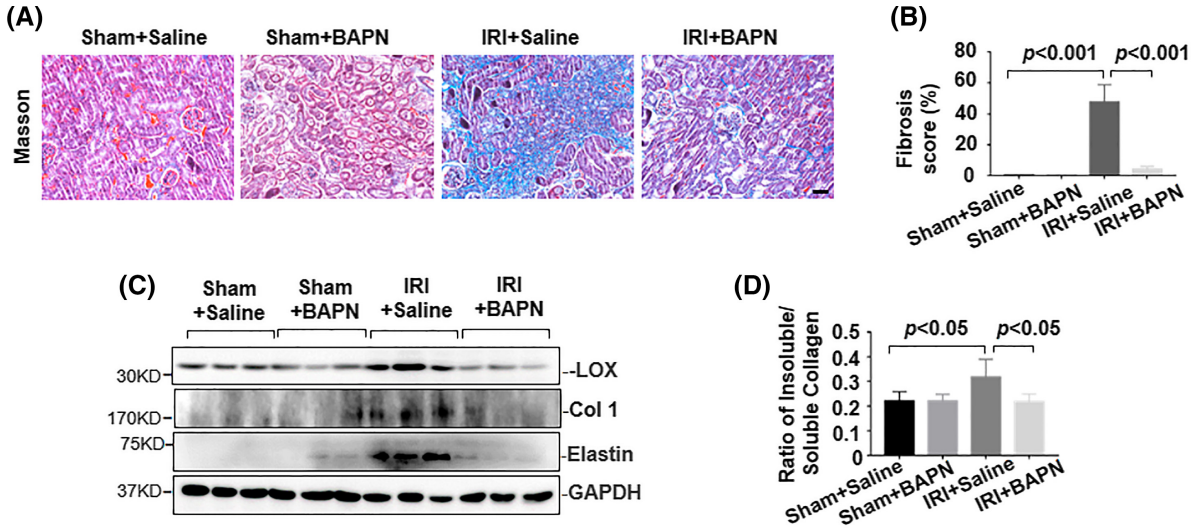

FIGURE 6 Targeting LOX using BAPN protects against renal fibrosis development. (A) Representative images of Masson's trichrome staining in kidney sections collected from mice with or without IRI injury treated with saline or BAPN. (B) The Masson trichrome-positive tubulointerstitial area (blue in C) relative to the whole area from 10 random cortical fields was analyzed. (C) Western blot analysis of the expression of LOX, Col1, and elastin in the kidney from mice with or without IRI injury treated with BAPN or saline. (D) The ratio of insoluble/soluble collagen was analyzed in mouse kidneys with or without IR-28d treated with BAPN or saline. Each bar represents the mean ± SEM for groups of at least 6 mice in vivo. The scale bar is 50 μm.

(extracellular matrix) in IRI kidneys was about 42.83% compared to that in control kidneys, whereas administration of BAPN significantly reduced ECM deposition by 64.63% (Figure 6B). Immunoblot analysis of whole-kidney tissue lysate indicated that administration of BAPN decreased the expression of LOX to the basal levels. Treatment with BAPN also significantly decreased the levels of elastin and collagen 1 in BAPN-treated IRI kidneys compared to saline-treated IRI kidneys (Figure 6C). Given that LOX catalyzes the proteolytic activation of the precursor of the collagen cross-linking, which increases matrix stiffness, we further examined the effects of BAPN on LOX-mediated matrix stiffness in IRI kidneys. As shown in Figure 6D, BAPN treatment decreased the overall ratio of insoluble to soluble collagen in the IRI kidneys compared to saline treatment (Figure 6E). The results that mice treated with BAPN inactivates LOX and decreased renal fibrosis after IRI injury reinforce the notion that LOX oxidase activity is essential in promoting IRI-induced renal fibrosis.

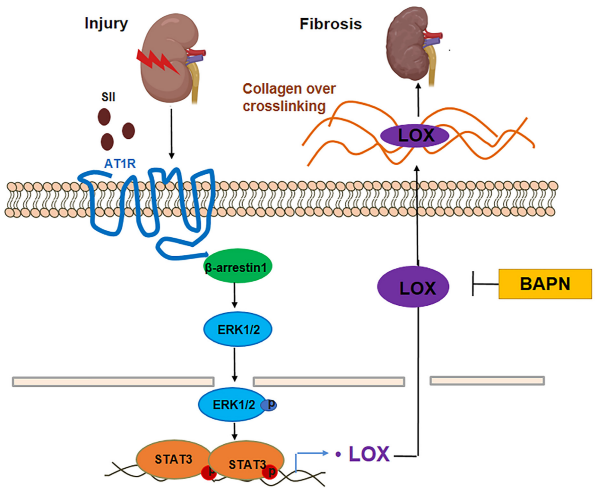

FIGURE 7 A diagram illustrating the mechanism by which upregulation of LOX promotes renal fibrosis. Injury to kidneys led to activation of β-arrestin/ERK biased signaling pathway and the downstream transcription factor STAT3 nuclear sublocation, which can bind to the promoter of LOX and increase its transcription, resulting in collagen over cross-linking. Targeting LOX with its inhibitor BAPN significantly suppressed IRI-induced collagen over cross-linking by decreasing LOX expression and activity, resulting in a decrease in renal fibrosis.

4 | DISCUSSION

LOX has been associated with aggressive cancers and metastasis,[7] however, the role and mechanism of LOX in renal fibrosis remains unknown. In this study, we show that upregulation of LOX contributes to ECM cross-linking and the progression of renal fibrosis in mouse kidneys with IRI. Targeting LOX with its inhibitor BAPN significantly decreased IRI-induced ECM over cross-linking by suppressing its expression and activity, resulting in a decrease in renal fibrosis. We further elucidated that ERK-STAT3 activation-mediated regulation of LOX expression was dependent on the AT1R-β-arrestin pathway (Figure 7).

In sum, this study suggests that ERK-STAT3 is the downstream of the AT1R-β-arrestin pathway and LOX may be a therapeutic target for the treatment of renal fibrosis.

β-arrestins are adaptor and signal transduction proteins that can form complexes with several signaling proteins, including the receptor tyrosine kinase (RTK) and the MAPK.[35] ERK signals activation mediated by β-arrestins has been found in some fibrotic diseases.[13,36] However, the downstream pathway mediated by β-arrestins-ERK in the process of fibrosis remains unknown. It has been shown that ERK-MAPK kinases regulate STAT3 activation in response to growth factors.[37] We found that STAT3 was significantly enriched in IRI fibrotic kidneys. STAT3 as a latent cytoplasmic transcription factor could transduce signals from the cell membrane to the nucleus upon tyrosine phosphorylation.[38] It has been reported that loss of β-arrestin1 affects STAT3 activation in T_H17 cells,[39] suggesting that the ERK-STAT3 pathway may be the downstream pathway of β-arrestin. To support this hypothesis, we performed nuclear-plasma separation in NRK-52E cells treated with SII, a selective agonist of β-arrestin. Importantly, we found that SII treatment activated ERK1/2 in the nucleus and later increased the phosphorylation of STAT3 at Try705 rather than at Ser727, whereas knockdown of β-arrestin1 or target ERK inhibited the phosphorylation of STAT3 at Tyr705 induced by SII, indicating that the phosphorylation of STAT3 at Tyr705 but not at Ser727 dependent on β-arrestin/ERK pathway. Moreover, it has been reported that the phosphorylation of STAT3 at Tyr705 in $Arrb1^{-/-}$ T cells were significantly attenuated while it could be enhanced by overexpression of β-arrestin1.[39] All these findings further support that STAT3 is downstream of β-arrestin1 and its activation at Tyr705 phosphorylation can be positively regulated by β-arrestin1 through scaffolding ERK cascade.

Most of the studies have indicated that the increase in ECM deposition and remodeling as well as structural changes in collagen contribute to the development of renal fibrosis.[40] Aberrant collagen cross-linking also resulted in a pathological microenvironment during the fibrosis process,[41] which largely depends on the enzymatic activity of LOX.[42] For example, angiotensin II treatment could induce an increase in the activity of LOX, which was accompanied by increased cross-linked collagen ratios and collagen content, leading to altered vascular stiffness.[43] In human lung tissues in ex vivo organ cultures, treatment with recombinant LOX resulted in an increasing hydroxyproline content and an induction of ECM components via upregulation of IL-6 and nuclear localization of c-Fos.[44] BAPN is a specific and irreversible inhibitor of LOX activity,[45] which acts through irreversibly binding to the LOX active site. This binding prevents LOX from catalyzing aldehyde formation and subsequently blocks the formation of new cross-links and the maturation of pre-existing immature cross-links.[46] It has been suggested that BAPN irreversibly blocks LOX enzyme activity, leading to the resynthesis and release of LOX.[47] In this study, we found that upregulation of LOX is responsible for the cross-linking collagen in IRI fibrotic kidneys and revealed that target LOX with BAPN not only reduced total collagen content but also the cross-linking collagen in those kidneys.

The regulation of LOX expression and activity with diverse mechanisms has been described in different cells and tissues from several species. In polycystic ovary syndrome, the AGE-mediated an increase in LOX mRNA and protein levels was due to the binding of the AGE-induced transcription factors NF-κB and activator protein-1 (AP-1) to the LOX promoter.[48] In an obesity-induced metabolic dysfunction model, the inhibition of LOX impacts adipocyte homeostasis and improves TNFα-induced insulin resistance.[49] In preterm premature membrane rupture, IL-1β activates the p38 and ERK1/2 pathways, which results in the activated NF-κB interacting with GATA3 at the NF-κB binding site of the LOX promoter to inhibit LOX expression.[50] By using the tool rVista 2.0, which predicts transcription factor binding, we found a conserved STAT3-binding site in the promoter region of the LOX, and the binding of STAT3 on the promoter of LOX was confirmed with ChIP assay. Thus, we identify that LOX is a direct target gene of STAT3 in renal fibrosis.

In summary, we demonstrate that LOX is upregulated in the chronically injured kidneys, which can be regulated by the AT1R-β-arrestin-ERK-STAT3-PY705 signaling pathway, and pharmacological inhibition of LOX with BAPN alleviates renal fibrosis by blocking LOX mediated collagen over cross-linking. It is necessary to demonstrate a universal function of LOX in mediating the pathology of CKD in a renal tubular cell type-specific knockout mice induced by diverse etiologies or other fibrotic diseases and delineate the translational potential of BAPN in clinical studies in the future.

ACKNOWLEDGMENTS

C. Yu was supported by grants from the National Natural Science Foundation of China (82170696 and 81873609). X.Li was funded by the National Institutes of Health R01 DK 129241 and R01 DK126662 grants.

AUTHOR CONTRIBUTIONS

Xiaoqin Zhang performed most experiments and data analysis. Wenqian Zhou, Yangyang Niu, and Saiya Zhu performed some of the experiments and data analysis. Yingying Zhang and Xiaogang Li assisted in data analysis and manuscript preparation. Chen Yu supervised the whole project, data analysis, and manuscript writing.

DISCLOSURES

The authors declare that they have no competing interests.

DATA AVAILABILITY STATEMENT

The data that support the findings of this study are available on request from the corresponding author. The data are not publicly available due to privacy or ethical restrictions.

ORCID

Chen Yu https://orcid.org/0000-0001-7169-276X

REFERENCES

1. He W, Dai C. Key Fibrogenic signaling. *Curr Pathobiol Rep*. 2015;3(2):183-192.
2. Xia J, He L-Q, Su X. Interventional mechanisms of herbs or herbal extracts on renal interstitial fibrosis. *J Integr Med*. 2016;14(3):165-173.
3. Cox TR, Bird D, Baker AM, et al. LOX-mediated collagen crosslinking is responsible for fibrosis-enhanced metastasis. *Cancer Res*. 2013;73(6):1721-1732.
4. Kumari S, Panda TK, Pradhan T. Lysyl oxidase: its diversity in health and diseases. *Indian J Clin Biochem*. 2017;32(2):134-141.
5. Wang TH, Hsia SM, Shieh TM. Lysyl oxidase and the tumor microenvironment. *Int J Mol Sci*. 2016;18(1):62.
6. Saatci O, Kaymak A, Raza U, et al. Targeting lysyl oxidase (LOX) overcomes chemotherapy resistance in triple negative breast cancer. *Nat Commun*. 2020;11(1):2416.
7. Barker HE, Cox TR, Erler JT. The rationale for targeting the LOX family in cancer. *Nat Rev Cancer*. 2012;12(8):540-552.
8. Chen L, Li S, Li W. LOX/LOXL in pulmonary fibrosis: potential therapeutic targets. *J Drug Target*. 2019;27(7):790-796.
9. Klepfish M, Gross T, Vugman M, et al. LOXL2 inhibition paves the way for macrophage-mediated collagen degradation in liver fibrosis. *Front Immunol*. 2020;11:480.
10. Zhang XQ, Li X, Zhou WQ, et al. Serum Lysyl oxidase is a potential diagnostic biomarker for kidney fibrosis. *Am J Nephrol*. 2020;51(11):907-918.
11. Marinissen MJ, Gutkind JS. G-protein-coupled receptors and signaling networks: emerging paradigms. *Trends Pharmacol Sci*. 2001;22(7):368-376.
12. Luttrell LM. Transmembrane signaling by G protein-coupled receptors. *Methods Mol Biol*. 2006;332:3-49.
13. Wang Y, Huang J, Liu X, et al. Beta-Arrestin-biased AT1R stimulation promotes extracellular matrix synthesis in renal fibrosis. *Am J Physiol Renal Physiol*. 2017;313(1):F1-F8.
14. Tan L, Yan W, McCorvy JD, Cheng J. Biased ligands of G protein-coupled receptors (GPCRs): structure-functional selectivity relationships (SFSRs) and therapeutic potential. *J Med Chem*. 2018;61(22):9841-9878.
15. Peterson YK, Luttrell LM. The diverse roles of Arrestin scaffolds in G protein-coupled receptor signaling. *Pharmacol Rev*. 2017;69(3):256-297.
16. Jean-Charles PY, Kaur S, Shenoy SK. G protein-coupled receptor signaling through beta-Arrestin-dependent mechanisms. *J Cardiovasc Pharmacol*. 2017;70(3):142-158.
17. DeWire SM, Kim J, Whalen EJ, Ahn S, Chen M, Lefkowitz RJ. Beta-arrestin-mediated signaling regulates protein synthesis. *J Biol Chem*. 2008;283(16):10611-10620.
18. Bologna Z, Teoh JP, Bayoumi AS, Tang Y, Kim IM. Biased G protein-coupled receptor signaling: new player in modulating physiology and pathology. *Biomol Ther (Seoul)*. 2017;25(1):12-25.
19. Tilley DG. G protein-dependent and G protein-independent signaling pathways and their impact on cardiac function. *Circ Res*. 2011;109(2):217-230.
20. Ahn S, Shenoy SK, Wei H, Lefkowitz RJ. Differential kinetic and spatial patterns of beta-arrestin and G protein-mediated ERK activation by the angiotensin II receptor. *J Biol Chem*. 2004;279(34):35518-35525.
21. McDonald PH, Chow CW, Miller WE, et al. Beta-arrestin 2: a receptor-regulated MAPK scaffold for the activation of JNK3. *Science*. 2000;290(5496):1574-1577.
22. Sun Y, Cheng Z, Ma L, Pei G. Beta-arrestin2 is critically involved in CXCR4-mediated chemotaxis, and this is mediated by its enhancement of p38 MAPK activation. *J Biol Chem*. 2002;277(51):49212-49219.
23. Li LX, Fan LX, Zhou JX, et al. Lysine methyltransferase SMYD2 promotes cyst growth in autosomal dominant polycystic kidney disease. *J Clin Invest*. 2017;127(7):2751-2764.
24. Dobin A, Davis CA, Schlesinger F, et al. STAR: ultrafast universal RNA-seq aligner. *Bioinformatics*. 2013;29(1):15-21.
25. Liao Y, Smyth GK, Shi W. featureCounts: an efficient general purpose program for assigning sequence reads to genomic features. *Bioinformatics*. 2014;30(7):923-930.
26. Robinson MD, McCarthy DJ, Smyth GK. edgeR: a Bioconductor package for differential expression analysis of digital gene expression data. *Bioinformatics*. 2010;26(1):139-140.
27. Yu G, Wang LG, Han Y, He QY. clusterProfiler: an R package for comparing biological themes among gene clusters. *OMICS*. 2012;16(5):284-287.
28. Zhou Y, Zhou B, Pache L, et al. Metascape provides a biologist-oriented resource for the analysis of systems-level datasets. *Nat Commun*. 2019;10(1):1523.
29. Cohen J. Weighted kappa: nominal scale agreement with provision for scaled disagreement or partial credit. *Psychol Bull*. 1968;70(4):213-220.
30. Luttrell LM. "Location, location, location": activation and targeting of MAP kinases by G protein-coupled receptors. *J Mol Endocrinol*. 2003;30(2):117-126.
31. Qi QR, Yang ZM. Regulation and function of signal transducer and activator of transcription 3. *World J Biol Chem*. 2014;5(2):231-239.
32. Smith-Mungo LI, Kagan HM. Lysyl oxidase: properties, regulation and multiple functions in biology. *Matrix Biol*. 1998;16(7):12-398.
33. Adam O, Theobald K, Lavall D, et al. Increased lysyl oxidase expression and collagen cross-linking during atrial fibrillation. *J Mol Cell Cardiol*. 2011;50(4):678-685.
34. Eishingdrelo H, Sun W, Li H, et al. ERK and beta-arrestin interaction: a converging point of signaling pathways for multiple types of cell surface receptors. *J Biomol Screen*. 2015;20(3):341-349.
35. Gu YJ, Sun WY, Zhang S, Wu JJ, Wei W. The emerging roles of beta-arrestins in fibrotic diseases. *Acta Pharmacol Sin*. 2015;36(11):1277-1287.
36. Xu H, Li Q, Liu J, et al. Beta-Arrestin-1 deficiency ameliorates renal interstitial fibrosis by blocking Wnt1/beta-catenin signaling in mice. *J Mol Med (Berl)*. 2018;96(1):97-109.

37. Chung J, Uchida E, Grammer TC, Blenis J. STAT3 serine phosphorylation by ERK-dependent and -independent pathways negatively modulates its tyrosine phosphorylation. *Mol Cell Biol*. 1997;17(11):6508-6516.
38. Darnell JE Jr. STATs and gene regulation. *Science*. 1997;277(5332):1630-1635.
39. Li J, Wei B, Guo A, et al. Deficiency of beta-arrestin1 ameliorates collagen-induced arthritis with impaired TH17 cell differentiation. *Proc Natl Acad Sci U S A*. 2013;110(18):7395-7400.
40. Niu YY, Zhang YY, Zhu Z, et al. Elevated intracellular copper contributes a unique role to kidney fibrosis by lysyl oxidase mediated matrix crosslinking. *Cell Death Dis*. 2020;11(3):211.
41. Cox TR, Erler JT. Remodeling and homeostasis of the extracellular matrix: implications for fibrotic diseases and cancer. *Dis Model Mech*. 2011;4(2):165-178.
42. Liu SB, Ikenaga N, Peng ZW, et al. Lysyl oxidase activity contributes to collagen stabilization during liver fibrosis progression and limits spontaneous fibrosis reversal in mice. *FASEB J*. 2016;30(4):1599-1609.
43. Eberson LS, Sanchez PA, Majeed BA, Tawinwung S, Secomb TW, Larson DF. Effect of lysyl oxidase inhibition on angiotensin II-induced arterial hypertension, remodeling, and stiffness. *PLoS One*. 2015;10(4):e0124013.
44. Nguyen XX, Nishimoto T, Takihara T, Mlakar L, Bradshaw AD, Feghali-Bostwick C. Lysyl oxidase directly contributes to extracellular matrix production and fibrosis in systemic sclerosis. *Am J Physiol Lung Cell Mol Physiol*. 2021;320(1):L29-L40.
45. Tang SS, Chichester CO, Kagan HM. Comparative sensitivities of purified preparations of lysyl oxidase and other amine oxidases to active site-directed enzyme inhibitors. *Connect Tissue Res*. 1989;19(1):93-103.
46. Canelon SP, Wallace JM. Beta-aminopropionitrile-induced reduction in enzymatic crosslinking causes in vitro changes in collagen morphology and molecular composition. *PLoS One*. 2016;11(11):e0166392.
47. Wuest M, Kuchar M, Sharma SK, et al. Targeting lysyl oxidase for molecular imaging in breast cancer. *Breast Cancer Res*. 2015;17:107.
48. Papachroni KK, Piperi C, Levidou G, et al. Lysyl oxidase interacts with AGE signalling to modulate collagen synthesis in polycystic ovarian tissue. *J Cell Mol Med*. 2010;14(10):2460-2469.
49. Miana M, Galán M, Martínez-Martínez E, et al. The lysyl oxidase inhibitor beta-aminopropionitrile reduces body weight gain and improves the metabolic profile in diet-induced obesity in rats. *Dis Model Mech*. 2015;8(6):543-551.
50. Zhang C, Wang W, Liu C, Lu J, Sun K. Role of NF-kappaB/GATA3 in the inhibition of lysyl oxidase by IL-1beta in human amnion fibroblasts. *Immunol Cell Biol*. 2017;95(10):943-952.

SUPPORTING INFORMATION

Additional supporting information can be found online in the Supporting Information section at the end of this article.

How to cite this article: Zhang X, Zhou W, Niu Y, et al. Lysyl oxidase promotes renal fibrosis via accelerating collagen cross-link driving by β-arrestin/ERK/STAT3 pathway. *The FASEB Journal*. 2022;36:e22427. doi: 10.1096/fj.202200573R